RSC Advances

COMMUNICATION

Anthracene/tetracene cocrystals as novel fluorophores in thin-film luminescent solar concentrators†

Cite this: *RSC Adv.*, 2014, **4**, 9893

Received 18th November 2013
Accepted 31st January 2014

DOI: 10.1039/c3ra46810k

www.rsc.org/advances

Gianmarco Griffini,* Luigi Brambilla, Marinella Levi, Chiara Castiglioni, Mirella Del Zoppo and Stefano Turri

Efficient thin-film luminescent solar concentrators (LSCs) were fabricated using tetracene-doped anthracene cocrystals as novel fluorescent systems dispersed in a poly(methyl methacrylate) matrix. The LSC device efficiency η_{LSC} was found to reach 2.50%, with an optical efficiency η_{opt} in excess of 23% and a concentration factor C of 0.83%.

Luminescent solar concentrators (LSCs) represent a promising technology to reduce manufacturing and installation costs of conventional photovoltaic (PV) systems.[1–3] In addition, LSCs may offer alternative solutions to some of the limitations given by standard silicon-based PV modules, such as their heavy weight, poor response under diffuse sunlight, and colors and shapes constraints.[3] In a typical device architecture, LSCs consist of a thin film of a transparent host matrix doped with one or more luminescent species deposited onto a transparent substrate, such as glass or plastic. Photons hitting the LSC surface are absorbed by the luminescent molecules and are re-emitted red-shifted. Because the refractive indices of the host matrix and the substrate are higher than that of air, a fraction of re-emitted photons is waveguided by total internal reflection to the edges of the waveguide, where it can be collected by small area PV cells.[4–6] Because LSCs can efficiently collect both direct and diffuse sunlight and thus do not require sun tracking systems, they are particularly interesting for building-integrated applications and for use in urban areas, where also their light weight and color tunability may offer interesting design and installation possibilities.[3,7,8]

Different transparent polymeric systems have been recently proposed as host matrices for thin film LSC devices,[9–13] with poly(methyl methacrylate) (PMMA) representing by far the most widely used because of its good optical properties (high transparency and high refractive index), easy processability and low cost.[14] As to the luminescent doping species, a great deal of work has been devoted to the development of luminophores that satisfy the main optical requirements to achieve highly efficient LSC devices, namely a broad absorption spectrum, a large Stokes shift, a high luminescence quantum yield and optimal matching between the emission spectrum of the luminophore and the spectral response of the PV cell. Following these guidelines, different promising luminescent species have been synthesized and incorporated in LSC devices, including organic dyes,[15–18] quantum dots[19,20] and inorganic phosphors/rare earth ions.[8,21,22] In particular, record device efficiencies in the range 4–7% have been achieved by employing rhodamine-, coumarin- or perylene-based organic dyes.[23–25] A fundamental issue common to all these systems is the need of achieving high levels of solubility of the luminescent species in the host matrix material during processing in order to obtain high device efficiencies. Poor dye solubility may lead to the formation of non-luminescent dimers and aggregates[26] that causes drop of fluorescence quantum yield and device performance. For this reason, appropriate choice of luminophore/host matrix combination is very important for optimal LSC device operations.

In the past few decades, organic crystals based on π-conjugated molecules have been extensively studied and employed in electronic devices such as field-effect transistors, lasers and PV cells, due to their high thermal stability, highly ordered molecular structure and high carrier mobility.[27,28] Recently,[29] organic molecular host/guest cocrystals based on anthracene (Ac) as the host material and tetracene (Tc) as the guest material have been prepared and have been shown to promote a very efficient host-to-guest energy transfer at very low concentrations of guest species due to the head-to-tail transition dipole alignment taking place upon crystal formation. Due to the very high Förster resonance energy transfer (FRET) efficiency of these systems, highly fluorescent films can also be obtained by doping a polymer solution with such molecular cocrystals and by using conventional wet processing techniques to deposit

Department of Chemistry, Materials and Chemical Engineering Giulio Natta, Politecnico di Milano, Piazza Leonardo da Vinci 32, 20133, Milano, Italy. E-mail: gianmarco.griffini@polimi.it

† Electronic supplementary information (ESI) available: Device fabrication and characterization, device performance evaluation, absorption and emission spectra, additional optical microscopy, *I–V* plot of Ac-only LSCs, spectral response of mc-Si PV cell. See DOI: 10.1039/c3ra46810k

luminescent doped films on appropriate substrates. Since in these cocrystals the guest molecule is the only responsible for the fluorescence emission and is present at very low concentrations compared to the host molecule, formation of non-luminescent aggregates is not expected. Therefore, these systems allow to overcome the limitations given by the need of high levels of solubility of the luminescent species (*viz.* organic dyes) in the carrier host matrix to achieve highly luminescent polymeric films.

In this work, we report the preparation of fluorescent films based on PMMA doped with Ac/Tc host/guest cocrystals and their use in LSC devices (Fig. 1a). To the best of our knowledge, this represents the first demonstration of the use of molecular cocrystals as fluorescent species in LSC devices. The fluorescent polymeric films were obtained by spin coating a solution of PMMA containing Ac and Tc onto glass substrate. By varying the solvent system, the processing temperature and the PMMA : (Ac/Tc) weight ratio, different cocrystal morphologies could be obtained that were found to influence the performance of the corresponding LSC devices. Optimized LSC devices with a geometric gain G of 3.5 were fabricated by coupling mc-Si PV cells to the four edges of the fluorescent PMMA-coated glass substrate. An absolute device efficiency η_{LSC} as high as 2.50% was found for our best LSC device, with an optical efficiency η_{opt} of 23.72% and a concentration factor C of 0.83% (see ESI† for details on definition of G, η_{LSC}, η_{opt} and C).

The normalized UV-vis absorption and fluorescence emission spectra of PMMA films doped with Ac/Tc cocrystals are presented in Fig. 1b. A PMMA : Ac : Tc = 1000 : 250 : 1 weight ratio was employed because it was previously shown[29] that an efficient host-to-guest FRET process can be achieved with such a low concentration of guest species. The absorption spectrum of the fluorescent film in the 300–450 nm region shows four distinct absorption peaks at 330 nm, 354 nm, 373 nm and 393 nm that can be attributed to the vibronic structure of pure Ac. On the other hand, the characteristic absorption features of Tc are not noticeable due to its very low concentration in the Ac/Tc-doped film (see ESI†). As opposed to this, the emission spectrum of the cocrystals is characterized by the quenching of the fluorescence of Ac (emission bands in the region 400–475 nm) and by the appearance of sharp emission bands in the 475–650 nm region that can be ascribed to the fluorescence of Tc (see ESI†). This behavior indicates a very efficient energy transfer between Ac and Tc in the doped polymeric film that allows for Tc molecules in the cocrystals to collect most of the excitation energy coming from the surrounding Ac molecules thus generating a strong Tc fluorescence emission. As already observed on single crystals,[29,30] this process is favored by the significant overlap between the emission spectrum of Ac and the absorption spectrum of Tc.

In the attempt to further characterize the host-to-guest energy transfer process and to evaluate the effect of film processing conditions on fluorescence emission, fluorescence spectra were collected on spin coated films deposited from different solvents at different processing temperatures. In particular, starting solutions of PMMA, Ac and Tc were prepared (PMMA : Ac : Tc = 1000 : 250 : 1 weight ratio) using four distinct solvents with good solubility for anthracene and tetracene but with different boiling temperatures (T_b) and chemical nature, namely chloroform ($CHCl_3$, T_b = 61 °C), toluene (TOL, T_b = 111 °C), chlorobenzene (CB, T_b = 130 °C) and 1,2-dichlorobenzene (DCB, T_b = 180 °C). The PMMA:Ac:Tc solutions were maintained at different temperatures (50 °C for $CHCl_3$, 100 °C for TOL and CB, 150 °C for DCB) overnight and then deposited hot onto glass substrates to form the fluorescent films. The fluorescence emission spectra of such thin films are presented in Fig. 2, where normalization with respect to the highest intensity emission peak was performed. An efficient energy

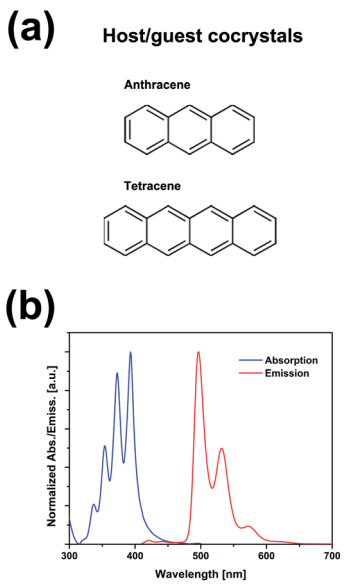

Fig. 1 (a) Molecular structures of the host/guest cocrystal materials employed in this work and (b) normalized absorption and emission spectra of a PMMA thin film doped with anthracene/tetracene cocrystals.

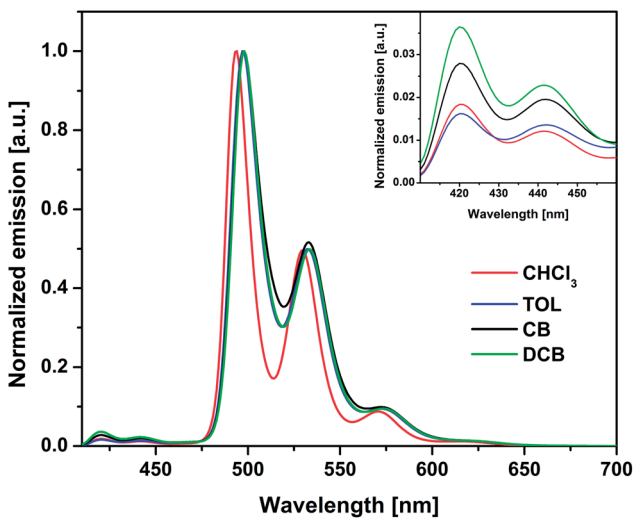

Fig. 2 Normalized fluorescence spectra of LSC thin films deposited from chloroform ($CHCl_3$), toluene (TOL), chlorobenzene (CB) and 1,2-dichlorobenzene (DCB) solution with PMMA : Ac : Tc = 1000 : 250 : 1. The inset shows a zoom of the 410–460 nm spectral region.

transfer from host molecule to guest molecule is observed in all systems, as evidenced by the emergence of a strong Tc emission in the 475–650 nm region. This behavior indicates that neither the type of solvent nor the processing temperature prevent the energy transfer process from occurring. As opposed to this, the intensity of the two peaks observed in all systems at 420 nm and 442 nm is found to be higher (about twice as high) for films deposited from DCB and CB compared to TOL and $CHCl_3$ (inset to Fig. 2). Since the emission peaks observed in the 400–460 nm spectral region are ascribed to the fluorescence of Ac (see ESI†), this behavior may indicate that the processing conditions (solvent and temperature) affect the degree of fluorescence quenching of Ac molecules in the cocrystals, the latter being closely related to the efficiency of the energy transfer process from Ac to Tc. In particular, a higher Ac fluorescence quenching (higher energy transfer efficiency) is found in systems obtained from $CHCl_3$ and TOL solutions compared to CB and DCB. In addition, the fluorescence spectra presented in Fig. 2 also show that the Tc emission peaks (475–650 nm) of films deposited from $CHCl_3$ solution are characterized by a 3 nm blue-shift compared to TOL, CB and DCB systems. Such hypsochromic shift may be ascribed to the effect of the solvent system on the morphology of Ac/Tc cocrystals in the PMMA:Ac:Tc thin film, as will be discussed in the following paragraph.

In order to further investigate the influence of film processing conditions on the size, shape and distribution of the Ac/Tc cocrystals forming in the PMMA films upon spin-coating, films cast from different solvents were also examined by means of optical microscopy. The results are presented in Fig. 3 for the $CHCl_3$, TOL, CB and DCB systems previously described. As shown in the micrographs, significantly larger features are observed when $CHCl_3$ is used compared to films deposited from other solvents. In particular, well defined long hexagonally-shaped microcrystals of increasing sizes can be clearly distinguished in the films deposited from $CHCl_3$ (Fig. 3a), with the largest being a few microns long. Conversely, cocrystals forming upon film deposition from TOL (Fig. 3b), CB (Fig. 3c) or DCB (Fig. 3d) all show a much finer dendritic morphology with significantly smaller randomly oriented crystals. The size of such crystals appears to increase slightly when going from TOL to CB to DCB systems. Such different crystal arrangement in the polymeric film ($CHCl_3$ compared to TOL, CB and DCB) may be explained by the effect of the crystal–solvent interactions on the solid–liquid interface during crystal formation, which is known to play a crucial role in determining the growth rate of crystal facets and thus in defining its final shape.[31,32] In particular, the stronger the interactions between the solvent and the crystal facet, the slower its growth rate. Due to the similar chemical structure, aromatic solvents such as TOL, CB and DCB manifest stronger interactions with anthracene (π–π stacking) compared to $CHCl_3$, thus partially hampering crystal growth. As opposed to this, long hexagonal crystals can form from $CHCl_3$ solution due to the poor solvent–crystal interactions. This different crystal morphology may also explain the slightly different spectral response found in films cast from $CHCl_3$, as discussed previously. Similar results were observed on analogous systems.[33] It is worth mentioning that no significant differences in crystal shape were found on films deposited from the same solvent at different processing temperatures (TOL at 50 °C and 100 °C, ESI†), further confirming the key role played by the solvent on the morphological arrangement of the cocrystals in the cast film.

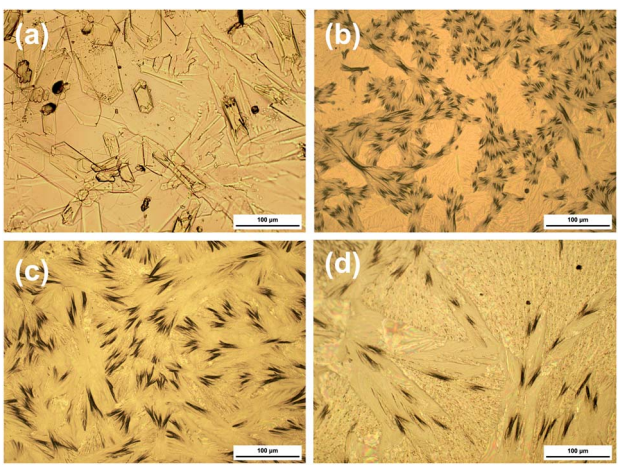

Fig. 3 Optical microscopy images (200× magnification) of LSC thin films deposited on glass slides from (a) $CHCl_3$, (b) TOL, (c) CB and (d) DCB solution with PMMA : Ac : Tc = 1000 : 250 : 1.

In order to evaluate the applicability of Ac/Tc cocrystals as fluorophores in LSC devices, thin PMMA films doped with Ac/Tc were spin-cast onto glass waveguides with serially-connected mc-Si PV cells attached to the four edges. *I–V* curves were recorded under AM1.5G solar irradiation (100 mW cm^{-2}). Following the previous discussion on the characterization of the energy transfer process on LSC films deposited from different solvents (Fig. 2), only LSC devices obtained from $CHCl_3$ and TOL solutions were tested, as these two systems were shown to allow for the most efficient quenching of Ac fluorescence (highest energy transfer efficiency) in the cocrystals. In addition, significantly different morphologies were observed on films cast from these two solvents (while TOL, CB and DCB gave comparable structures), thus allowing to evaluate the effect of crystal morphology and arrangement on device performance. The results of PV characterization of LSC devices are reported in Fig. 4a, where the *I–V* curves of all systems are presented. In addition to varying solvent system, the effect of film thickness (by varying spin coating speed) and of PMMA : fluorophore ratio (PMMA : Ac : Tc = 1000 : 250 : 1 *vs.* PMMA : Ac : Tc = 750 : 250 : 1) on the performance of LSC devices was also investigated, and the resulting device parameters are summarized in Table 1. No significant differences are observed by varying the polymer : fluorophore ratio on LSC devices obtained from $CHCl_3$ solution, as in both cases (B-$CHCl_3$ and C-$CHCl_3$ LSC devices) efficiencies in the order of 2.30% are obtained, with comparable values of η_{opt} (21.20% and 21.44) and *C* (0.74 and 0.75). On the other hand, the effect of the polymer : fluorophore ratio on LSC device performance is more pronounced in devices obtained from TOL solution, where a maximum η_{LSC} = 2.50% is obtained for devices with a PMMA : Ac : Tc = 1000 : 250 : 1 ratio (B-TOL), together with a

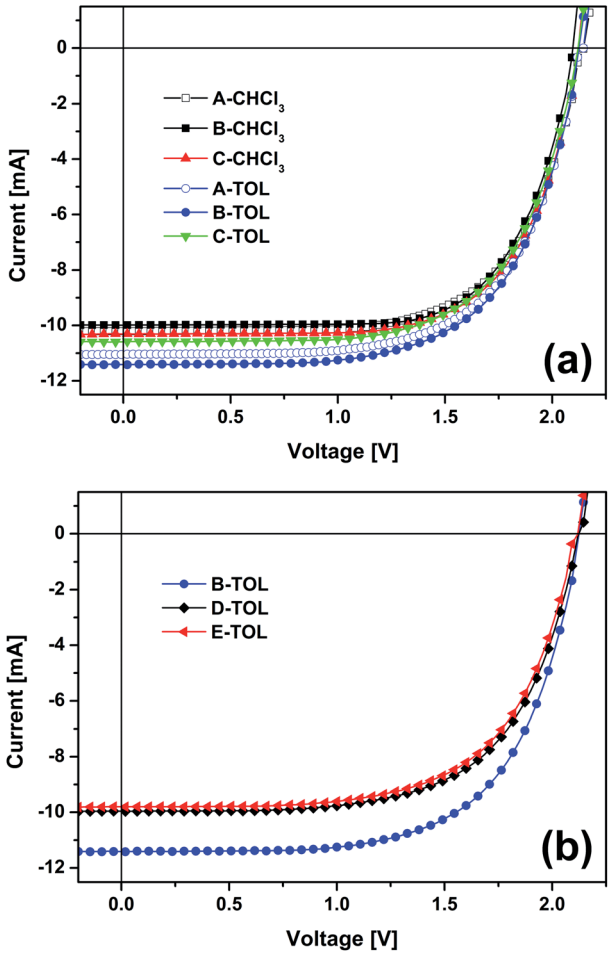

Fig. 4 Current–voltage (I–V) curves of (a) LSC devices deposited from $CHCl_3$ or TOL solution at varying spin coating speed (600 rpm for B-$CHCl_3$, C-$CHCl_3$, B-TOL and C-TOL, 1200 rpm for A-$CHCl_3$ and A-TOL) and with varying PMMA : Ac : Tc ratio (1000 : 250 : 1 for A-$CHCl_3$, B-$CHCl_3$, A-TOL and B-TOL, 750 : 250 : 1 for C-$CHCl_3$ and C-TOL) and (b) LSC devices deposited from TOL with varying Ac : Tc ratio (250 : 1, 250 : 5, 250 : 10 for C-TOL, D-TOL and E-TOL, respectively).

Table 1 LSC device parameters (device efficiency η_{LSC}, optical efficiency η_{opt} and concentration factor C) obtained under AM 1.5G irradiation (100 mW cm^{-2}) for the systems considered in this work. Processing conditions for each device have also been reported ($CHCl_3$ – chloroform, TOL – toluene)

LSC device[a]	PMMA : Ac : Tc	Spin coating speed rpm	η_{LSC} %	η_{opt} %	C
A-$CHCl_3$	1000 : 250 : 1	1200	2.28	21.42	0.75
B-$CHCl_3$	1000 : 250 : 1	600	2.30	21.44	0.75
C-$CHCl_3$	750 : 250 : 1	600	2.33	21.20	0.74
A-TOL	1000 : 250 : 1	1200	2.44	22.60	0.79
B-TOL	1000 : 250 : 1	600	2.50	23.72	0.83
C-TOL	750 : 250 : 1	600	2.33	21.97	0.77
D-TOL	1000 : 250 : 5	600	2.15	19.78	0.68
E-TOL	1000 : 250 : 10	600	2.10	19.87	0.69
Ac-only	1000 : 250 : 0	600	1.03	12.21	0.42

[a] Geometric gain G for all LSC devices is 3.5.

η_{opt} value as high as 23.72% and $C = 0.83$. By increasing spin coating speed from 600 rpm to 1200 rpm, no major modifications are observed in terms of device efficiency, indicating a negligible influence of film thickness on device performance for the values of thicknesses examined in this work (see ESI†). These results may be explained by considering the different morphologies of the Ac/Tc cocrystals in the LSCs forming upon film deposition from different solvents. The long hexagonal crystals with face-on orientation observed in LSC films deposited from $CHCl_3$-based solutions may yield anisotropic polarized fluorescence emission. As opposed to this, the smaller randomly oriented cocrystals forming in films cast from TOL solution may guarantee a higher level of emission isotropicity. These effects may influence photon trapping and transport efficiencies and in turn the overall efficiency of the LSC device. Another concurrent effect may be related to the surface roughness of the LSC films that is found to be larger for films deposited from $CHCl_3$ solution and for PMMA : Ac : Tc = 750 : 250 : 1 ratios. In particular, surface root-mean-square roughness values of 1.98 μm, 2.56 μm, 0.43 μm and 0.85 μm are found for B-$CHCl_3$, C-$CHCl_3$, B-TOL and C-TOL LSC devices, respectively. The increased roughness may be responsible for an increased loss of photons due to undesired front face reflection that yields lower LSC device efficiencies.

To evaluate the influence of the host–guest proportions in the deposited film on device performance, LSCs with Ac : Tc ratios of 250 : 1 (B-TOL device), 250 : 5 (D-TOL device) and 250 : 10 (E-TOL device) were also prepared and tested. As shown in the I–V plot presented in Fig. 4b and from the corresponding device parameters listed in Table 1, by increasing the concentration of guest molecule, a decrease of LSC device performance is observed. In particular, η_{opt} values lower than 20% are obtained for both 250 : 5 and 250 : 10 Ac : Tc ratios. These results are in agreement with recent literature reports,[29] in which a reduction of host-to-guest energy transfer efficiency was found by decreasing the Ac : Tc ratio in the deposited polymeric film. Such lower energy transfer efficiency may be responsible for a decrease of photons emitted by Tc and made available to the PV cell for the photon-to-electricity conversion, with a consequent decrease of LSC device performance.

To further characterize the PV behavior of these systems, also Ac-only LSC devices were fabricated and tested (see ESI† for I–V plot). As reported in Table 1, a significant increase in device performance is obtained by employing host–guest Ac:Tc cocrystals in the polymeric LSC film compared to Ac-only devices ($\eta_{opt} = 12.21\%$ and $\eta_{opt} = 23.72\%$ for Ac-only and Ac:Tc (B-TOL) devices, respectively). These results indicate that the highly efficient Ac-to-Tc energy transfer process in the cocrystals at very low Tc concentration combined with the red-shifted emission of Tc *vs.* Ac allow for a more favorable light management in the LSC system compared to Ac-only devices. In addition, it is worth mentioning that Tc-only LSC devices were also prepared and tested (PMMA : Ac : Tc = 1000 : 0 : 1) but no appreciable device efficiency was reported ($\eta_{LSC} < 10^{-2}\%$). This result may be explained by the negligible fluorescence emission observed in PMMA:Tc films with concentration values of Tc as low as those used in the cocrystals.

Although direct comparisons are made difficult by the strong dependence of device efficiency on several parameters related to LSC device configuration such as dimensions, number and type of solar cells attached and device architecture, it is worth noticing that the η_{LSC}, η_{opt} and C values obtained in this work for Ac/Tc-based LSCs are comparable to those found in the literature on systems employing organic dyes.[24] Even though the spectral match between Ac/Tc absorption and solar emission and between Ac/Tc emission and mc-Si PV cell response (ESI†) is far from being optimal, these systems represent a promising platform to achieve high efficiency LSC devices.

Conclusions

In conclusion, fluorescent films based on PMMA containing Ac/Tc cocrystals were prepared and employed in thin-film LSC devices. Process optimization yielded LSC systems with a device efficiency η_{LSC} as high as 2.50%, an optical efficiency η_{opt} of 23.72% and a concentration factor C of 0.83%. The effect of solvent system and processing temperature as well as of the PMMA : fluorophore and Ac : Tc weight ratios was also investigated and these parameters were found to influence cocrystal morphology and in turn device efficiency. This first demonstration of the use of molecular cocrystals as novel fluorescent species in LSC devices opens up new strategies for the preparation of efficient fluorophores for LSC applications. In addition, due to the higher photostability of molecular crystals compared to common organic dyes, LSC device lifetime is also expected to benefit from their use.

Notes and references

1 M. J. Currie, J. K. Mapel, T. D. Heidel, S. Goffri and M. A. Baldo, *Science*, 2008, **321**, 226–228.
2 J. Yoon, L. F. Li, A. V. Semichaevsky, J. H. Ryu, H. T. Johnson, R. G. Nuzzo and J. A. Rogers, *Nat. Commun.*, 2011, **2**, 343.
3 M. G. Debije and P. P. C. Verbunt, *Adv. Energy Mater.*, 2012, **2**, 12–35.
4 G. Smestad, H. Ries, R. Winston and E. Yablonovitch, *Sol. Energy Mater.*, 1990, **21**, 99–111.
5 U. Rau, F. Einsele and G. C. Glaeser, *Appl. Phys. Lett.*, 2005, **87**, 171101.
6 D. J. Farrell and M. Yoshida, *Prog. Photovoltaics*, 2012, **20**, 93–99.
7 G. Kocher-Oberlehner, M. Bardosova, M. Pemble and B. S. Richards, *Sol. Energy Mater. Sol. Cells*, 2012, **104**, 53–57.
8 Y. Zhao and R. R. Lunt, *Adv. Energy Mater.*, 2013, **3**, 1143–1148.
9 V. Fattori, M. Melucci, L. Ferrante, M. Zambianchi, I. Manet, W. Oberhauser, G. Giambastiani, M. Frediani, G. Giachi and N. Camaioni, *Energy Environ. Sci.*, 2011, **4**, 2849–2853.
10 Y. S. Lim, C. K. Lo and G. B. Teh, *Renewable Energy*, 2012, **45**, 156–162.
11 M. Buffa, S. Carturan, M. G. Debije, A. Quaranta and G. Maggioni, *Sol. Energy Mater. Sol. Cells*, 2012, **103**, 114–118.
12 G. Griffini, M. Levi and S. Turri, *Sol. Energy Mater. Sol. Cells*, 2013, **118**, 36–42.
13 G. Griffini, M. Levi and S. Turri, *Prog. Org. Coat.*, 2014, **77**, 528–536.
14 W. G. J. H. van Sark, K. W. J. Barnham, L. H. Slooff, A. J. Chatten, A. Buchtemann, A. Meyer, S. J. McCormack, R. Koole, D. J. Farrell, R. Bose, E. E. Bende, A. R. Burgers, T. Budel, J. Quilitz, M. Kennedy, T. Meyer, C. D. M. Donega, A. Meijerink and D. Vanmaekelbergh, *Opt. Express*, 2008, **16**, 21773–21792.
15 G. Seybold and G. Wagenblast, *Dyes Pigm.*, 1989, **11**, 303–317.
16 O. A. Bozdemir, S. Erbas-Cakmak, O. O. Ekiz, A. Dana and E. U. Akkaya, *Angew. Chem., Int. Ed.*, 2011, **50**, 10907–10912.
17 G. Griffini, L. Brambilla, M. Levi, M. Del Zoppo and S. Turri, *Sol. Energy Mater. Sol. Cells*, 2013, **111**, 41–48.
18 A. Sanguineti, M. Sassi, R. Turrisi, R. Ruffo, G. Vaccaro, F. Meinardi and L. Beverina, *Chem. Commun.*, 2013, **49**, 1618–1620.
19 J. Bomm, A. Buchtemann, A. J. Chatten, R. Bose, D. J. Farrell, N. L. A. Chan, Y. Xiao, L. H. Slooff, T. Meyer, A. Meyer, W. G. J. H. van Sark and R. Koole, *Sol. Energy Mater. Sol. Cells*, 2011, **95**, 2087–2094.
20 F. Purcell-Milton and Y. K. Gun'ko, *J. Mater. Chem.*, 2012, **22**, 16687–16697.
21 O. Moudam, B. C. Rowan, M. Alamiry, P. Richardson, B. S. Richards, A. C. Jones and N. Robertson, *Chem. Commun.*, 2009, 6649–6651.
22 G. Katsagounos, E. Stathatos, N. B. Arabatzis, A. D. Keramidas and P. Lianos, *J. Lumin.*, 2011, **131**, 1776–1781.
23 L. H. Slooff, E. E. Bende, A. R. Burgers, T. Budel, M. Pravettoni, R. P. Kenny, E. D. Dunlop and A. Buchtemann, *Phys. Status Solidi RRL*, 2008, **2**, 257–259.
24 J. C. Goldschmidt, M. Peters, A. Bosch, H. Helmers, F. Dimroth, S. W. Glunz and G. Willeke, *Sol. Energy Mater. Sol. Cells*, 2009, **93**, 176–182.
25 L. Desmet, A. J. M. Ras, D. K. G. de Boer and M. G. Debije, *Opt. Lett.*, 2012, **37**, 3087–3089.
26 K. A. Colby, J. J. Burdett, R. F. Frisbee, L. Zhu, R. J. Dillon and C. J. Bardeen, *J. Phys. Chem. A*, 2010, **114**, 3471–3482.
27 J. S. Brooks, *Chem. Soc. Rev.*, 2010, **39**, 2667–2694.
28 A. A. Virkar, S. Mannsfeld, Z. Bao and N. Stingelin, *Adv. Mater.*, 2010, **22**, 3857–3875.
29 H. Wang, B. L. Yue, Z. Q. Xie, B. R. Gao, Y. X. Xu, L. L. Liu, H. B. Sun and Y. G. Ma, *Phys. Chem. Chem. Phys.*, 2013, **15**, 3527–3534.
30 H. P. Li, L. Duan, D. Q. Zhang, G. F. Dong, L. D. Wang and Y. Qiu, *Sci. China, Ser. B: Chem.*, 2009, **52**, 181–187.
31 M. Lahav and L. Leiserowitz, *Chem. Eng. Sci.*, 2001, **56**, 2245–2253.
32 H. P. Li, D. Q. Zhang, L. A. Duan, G. F. Dong, L. D. Wang and Y. Qiu, *Jpn. J. Appl. Phys., Part 1*, 2007, **46**, 7789–7792.
33 E. tenGrotenhuis, J. C. vanMiltenburg and J. P. vanderEerden, *Chem. Phys. Lett.*, 1996, **261**, 558–562.